EPJ Photovoltaics **15**, 20 (2024)

https://doi.org/10.1051/epjpv/2024014

Available online at:
www.epj-pv.org

ORIGINAL ARTICLE OPEN ACCESS

Comparative life cycle assessment of different fabrication processes for perovskite solar mini-modules

Federico Rossi[1,a], Leonardo Rotondi[1,a], Maurizio Stefanelli[2], Adalgisa Sinicropi[1,3,4], Luigi Vesce[2,*], and Maria Laura Parisi[1,3,4,**]

[1] University of Siena, R[2]ES Lab, Department of Biotechnology, Chemistry and Pharmacy, Via Aldo Moro 2, Siena, Italy
[2] CHOSE – Centre for Hybrid and Organic Solar Energy, Department of Electronic Engineering, University of Rome "Tor Vergata", Via del Politecnico 1, 00133 Rome, Italy
[3] CSGI, Center for Colloid and Surface Science, Via della Lastruccia 3, 50019 Sesto Fiorentino, Italy
[4] ICCOM-CNR, Institute of Chemistry of Organometallic Compounds, Consiglio Nazionale delle Ricerche, Via Madonna del Piano 10, 50019 Sesto Fiorentino, Italy

Received: 29 September 2023 / Accepted: 20 March 2024

Abstract. Sustainable energy production is one of the major goals for society to address climate change, with the aim of reducing fossil fuel consumption and greenhouse gases emissions. One of the main alternatives to burning fossil fuels is solar energy conversion; therefore, scientific research has moved towards the development of photovoltaic devices that are able to harvest solar radiation and convert it into electric energy, such as perovskite solar cells (PSCs). Several production processes for PSCs exist, differing in the deposition technique of PSCs layers as well as energy and material consumption. One of the main challenges is then to minimize the environmental impact of PSC manufacturing, which can be assessed through Life Cycle Assessment. The aim of this work is to evaluate and compare the eco-profiles of four different PSC production line at mini-module scale, namely, Spin Coating, Blade Coating, Spin Coating + Press and Blade Coating in Glovebox. Results disfavour the latter manufacturing route, showing that its burden is higher than the alternatives. Differently, the Blade Coating process results to be the one having the lowest environmental impact among the proposed solutions, whereas Spin Coating and Spin Coating + Press lines show almost the similar intermediate result.

Keywords: Life Cycle Assessment / LCA / perovskite solar cells / blade coating / spin coating / module

1 Introduction

The main source of energy that is used to produce electricity worldwide is currently the combustion of fossil resources in centralized thermoelectric power plants. According to the international agreements for climate and to the energy policies promoted by most of the countries, fossil fuels consumption shall be diminished to mitigate greenhouse gas (GHG) emissions and global warming effects towards a green energy transition [1–4]. One of the most attractive solutions to produce low-carbon electricity is represented by novel technologies for the conversion of solar energy, that is widely distributed all over the planet, abundant and almost inextinguishable [5–7]. However, although solar energy technologies do not imply direct emissions of GHG during operation, they determine environmental burdens along with their manufacturing chain [8,9]. For such reason, the production of solar panels requires energy, that can be produced from both renewable and fossil resources; this issue can strongly affect the environmental burden of solar panels, especially when they are produced in countries that are powered by carbon intensive electricity production mixes (i.e. China, that is currently the main producer of PV cells) [10,11]. Also, all the materials employed for the construction of solar energy technologies are subject to extraction, transport and transformation processes that determine the release of GHG and other pollutants. Moreover, the depletion of natural resources (i.e. fossil fuels, minerals, metals, water and land) and the emission of several pollutants to the environment also represent concerning environmental issues as well as GHG emissions. Therefore, in principle, all renewable energy conversion systems can be responsible for relevant environmental burdens, and the production of environmentally friendly solar energy harvesting devices is one of the main challenges. Accordingly, Life Cycle Assessment (LCA) is one of the main methodologies allowing for an early-stage evaluation of all the

* e-mail: vesce@ing.uniroma2.it
** e-mail: marialaura.parisi@unisi.it
[a] These authors contributed equally to this work.

above-mentioned environmental issues as it considers the whole life cycle of the process, including the manufacturing of solar cells [12,13].

Today, one of the most promising technologies is the perovskite solar cell (PSC): these devices contain a photoactive material called perovskite (PSK); after several years of research and development, these cells are now considered as very competitive in terms of economic convenience, thanks to the adopted low-cost printing techniques, and energy efficiency due to their high absorption coefficient and charge carrier mobility [14–18]. Moreover, PSC technology efficiencies reached values up to 26.1% for the single junction and 33.7% in tandem with silicon in a decade [19]. The high efficiency of PSCs is expected to further increase and it represents the main advantage compared to alternative PV technologies such as crystalline silicon cells (whose efficiency is currently around 26%) [14–18]. Moreover, the PSCs' characteristic of being coloured and semi-transparent make them suitable for more applications compared to silicon modules, especially in the buildings sector [20–22].

PSCs are made of several layers that are deposited one onto the others on top of a TCO (Transparent Conductive Oxide) covered flexible or rigid substrate, which can also be used as a counter electrode. The PSK layer is in between a p-type (HTL, Hole Transporting Layer) and n-type (ETL, Electron Transporting Layer) material to improve the charge extraction from the absorber [15,23]. A metal (Au, Ag, Cu) or a carbon-based material acts as counter-electrode [24]. The fabrication processes differ in the techniques employed for layers deposition and thus for the raw materials (i.e. solvents) and for the energy demanded by the manufacturing process. PSK film fabrication processes can be divided into two categories: one-step and two-step [25,26]. In one-step processes PSK layer is formed by nucleation and growth process of a solution containing all the precursors; this process is usually assisted by heating and subsequent evaporation of solvents. Two-step processes are characterized by different deposition steps for each different precursors (i.e. lead (Pb) halide or lead based adduct and liquid, vapour or solid organic salt) and PSK formation assisted by thermal treatment; precise reaction path of this process has been described [27]. PSK film formation methods can be further classified into solution-based and vapor-based [28]. Solution-based techniques comprehend spin coating, meniscus coating, spray coating and inkjet printing. In the spin coating process, precursor solution is dropped over the substrate that is subsequently rotated at a controlled velocity in order to spread the solution evenly. Blade, bar and slot-die coating techniques are kinds of meniscus coating, where a coating tool is used to spread the material over the substrate. In the case of the slot-die the solution is continuously distributed through a feed slot between the two dyes. The spray coating process involves spraying a mist of precursor solution onto the substrate and can be pressure-assisted, electro-assisted and sonication-assisted. In the inkjet printing method, the precursor solution is deposited onto the substrate in the form of ink droplets, and subsequently dried. Vapour-based techniques include thermal vacuum deposition, Chemical Vapour Deposition (CVD) and Hybrid Chemical Vapour Deposition (HCVD). Thermal vacuum deposition consists of vaporizing sources in vacuum and then depositing them onto the substrate; it is usually used for metals or inorganic salts. CVD exploits the reaction of one or more gas reactants leading to the formation of the desired film on the substrate and it is usually used for organic salts. HCVD mixes these latter techniques combining a thermal vacuum deposition for inorganic salts and CVD for organic ones; the two vapours will then react, forming the film perovskite onto the substrate [23,26,29,30]. The described methods play a fundamental role in the upscaling from lab-scale cells to modules of the PSC technology to obtain reproducible and homogeneous layers [31,32]. A module is the interconnection in series or in parallel of a number of cells to mitigate the sheet resistance of the conductive substrates [33,34].

The existence of different fabrication processes for PSK solar energy systems entails that their sustainability depends on the environmental impact of the fabrication techniques that are employed to produce it. Useful methodological guidelines to perform a LCA in the photovoltaics sector are available from Frischknecht et al. [35] and Wade et al. [36]. Moreover, several studies published in the scientific literature employ LCA methodology to assess the environmental impact of PSK solar energy systems. Zhang et al. [37] evaluated the environmental burdens of 5 PSC architectures, differing in the PSK layer composition: methylammonium tin triiodide ($MASnI_{3-x}Br_x$), methylammonium lead iodide ($MAPbI_3$), formamidinium lead iodide ($FAPbI_3$), cesium lead iodide ($CsPbI_3$) and methylammonium lead iodide chloride ($MAPbI_2Cl$). They performed LCA both "from cradle to gate" and "from cradle to grave" stating that $MAPbI_3$ and $FAPbI_3$ have the largest environmental impact comparing 1 cm^2 of active area, due to higher amounts of solvents used. Considering the production of 1 kWh as functional unit, results strongly depend on the relative conversion efficiencies of the cells. The manufacturing phase results to have the largest environmental impact among all the others, mostly due to gold production and solvent use for cleaning. Such impact can be reduced by substituting gold with silver or aluminium for counter-electrode contacts, and recycled solvents for fresh ones. Furthermore, tin and lead, although being of great concern particularly for their diffusion in the environment [38], are assessed as just minor factors influencing the overall eco-profile of the cell according to the authors, because they represent a small portion within the bill of materials [37]. Alberola-Borràs et al. [39] applied a "from cradle to grave" LCA to four different PSCs devices, considering $MAPbI_3$ as photoactive layer deposited following different procedures. They are spin coating of $PbCl_2$ and MAI 1:3 solution (Device 1), spin coating of PbI_2 and MAI 1:1 solution (Device 2), dipping of a spin coated PbI_2 film into a MAI solution (Device 3) and spin coating of PbI_2 and MAI 1:1 solution but with a mesoporous TiO_2 scaffold instead of the planar one (Device 4). Results show that the issues of the production process were the ones in common among the four analysed systems. Moreover, Devices 1 and 2 are the most eco-friendly, while Devices 3 and 4 can compete only if they have high efficiency and stability long enough to overcome

production costs. On the other hand, Device 4, thanks to its architecture, seems to be the most benefitting from a recycling end of life scenario [39]. Okoroafor et al. [40] performed a "from cradle to gate" LCA on a PSK produced exploiting the inkjet printing materials deposition method and comparing it with the spin coating fabrication. They also investigated the consequences of substituting the solvents usually used with a novel type of green solvent, i.e. eliminating dimethylformamide (DMF). Researchers found out that the major contribution to the environmental impact is the electricity consumption. Employed materials also play a key role due to the use of silver as back contact. In addition, scientists stated that, among all layers, the one contributing the most to the overall impact is the HTL, since it accounts for the 72% of the total used energy. Furthermore, according to the results, the use of DMF-free solvent significantly improved the eco-profile of the device, and the inkjet printing method shows a lower burden than the spin coating, due to lower electricity consumption and higher efficiency [40]. Krebs-Moberg et al. [41] evaluated and compared the environmental impact of three different type of solar cells, namely multi-crystalline silicon (m-Si), organic (OSC) and inorganic photovoltaic cells through a "from cradle to grave" LCA, investigating different end of life scenarios. Results indicate that m-Si solar module is the device with the highest environmental impact, due almost entirely to the energy consumed during the manufacturing process of the silicon wafers [41]. The above-mentioned literature studies are focused on small size PV modules; the issues associated with solar cell size upscaling has been addressed by Vesce et al. [42] with an LCA perspective. Such study demonstrates that scaling up the size of mini-modules to sub-modules allows enhancing the resource efficiency of their manufacturing, and, thus, the overall eco-profile of PSK devices. However, according to Vesce et al. [42], if the material architecture of the module remains the same, there are other environmental burdens that are not mitigated by the scaling up; this is the case, for example, when considering the percentage impact contribution of gold in PSK sub-modules at the characterization level that is overall higher than in small PV mini-modules.

In this study we selected some of the PSK manufacturing processes among those mentioned in the introductory remarks, based on the suitability and representativeness of the data inventories reported. When needed, the data extracted from the selected studies have been integrated with primary information provided by the Centre for Hybrid and Organic Solar Energy (CHOSE) to develop robust LCA models for different manufacturing techniques that can be considered as alternative solutions to fabricate one PSK mini-module. The aim of this work is to compare the eco-profiles of such production processes, selected based on LCA data availability, and to provide detailed data regarding energy and material consumptions, thus attempting to fill the literature gap in this regard.

Although LCA of PSK cells is a topic already discussed in the literature, a consistent LCA comparison among several techniques to produce the same PSK solar device has not been considered as a specific focus so far. As demonstrated by the literature review presented in the previous paragraphs, the studies published by previous scientists are strongly materials-focused and they are mostly aimed to the impact assessment and the comparison of different PSK cells architectures. On the other hand, to the best of our knowledge, the fabrication techniques (extensively described in Sect. 2) have never been compared in the literature using a LCA perspective. Given this context, a direct comparison with the results obtained in other LCA analyses available in the scientific literature is out of the scope of this study because such comparison would be affected by several methodological inconsistencies as described in the Supporting Information. Moreover, the literature lacks transparent and reproducible life cycle datasets for the environmental evaluation of PSK solar devices.

2 Description of the analysed system

This section contains the description of all the manufacturing techniques that are considered for comparison in this study. In particular, four manufacturing routes will be compared, namely Spin Coating, Blade Coating, Spin Coating + Press and Blade Coating in Glovebox.

The first fabrication step is the P1 scribing used to insulate the different cells on the TCO. Cleaning substrate is the next step made with ultrasonic bath in solvents with different polarity (Acetone, Ethanol, Isopropanol). All the considered works adopted the mesoscopic n-i-p structure: first compact TiO_2 and then mesoscopic TiO_2 were deposited through spray pyrolysis at 450 °C and spin/blade coating followed by 500 °C annealing, respectively. After ETL, perovskite deposition is carried out with different approaches according to the precursor, the ambient deposition and the deposition technique (see next paragraph). The deposition of the hole transport material with blade or spin coating is the last step before P2 laser process, where the entire stack is removed till TCO to guarantee the vertical series connection between the cells. Finally, gold is evaporated in high vacuum chamber and P3 process complete the device patterning with the metal contact etching. The described steps are depicted in Figure 1. Taking as a reference the Spin Coating process, identical steps are highlighted in green, while different characterizing steps are highlighted in red. More specifically, characterizing steps are the ones devoted to the deposition of HTL, ETL and the photoactive PSK layers. Moreover, the process "Blade Coating in Glovebox" presents differences also in the Cleaning step.

Such mini-modules manufacturing processes, whose architectures are graphically represented in Figure 2, are labelled referring to the PSK layer deposition methods adopted:

- "Spin Coating" [43]: the layers deposition is made using the spin coating technique, namely pouring the perovskite precursor solution onto the glass substrate and rotating it at a certain velocity in order to spread evenly the solution. An annealing step follows to dry the film. This process is carried out in a N_2 environment glovebox.
- "Blade Coating" [43]: the layers deposition is made using the blade coating technique, namely depositing the perovskite precursor solution onto the glass substrate

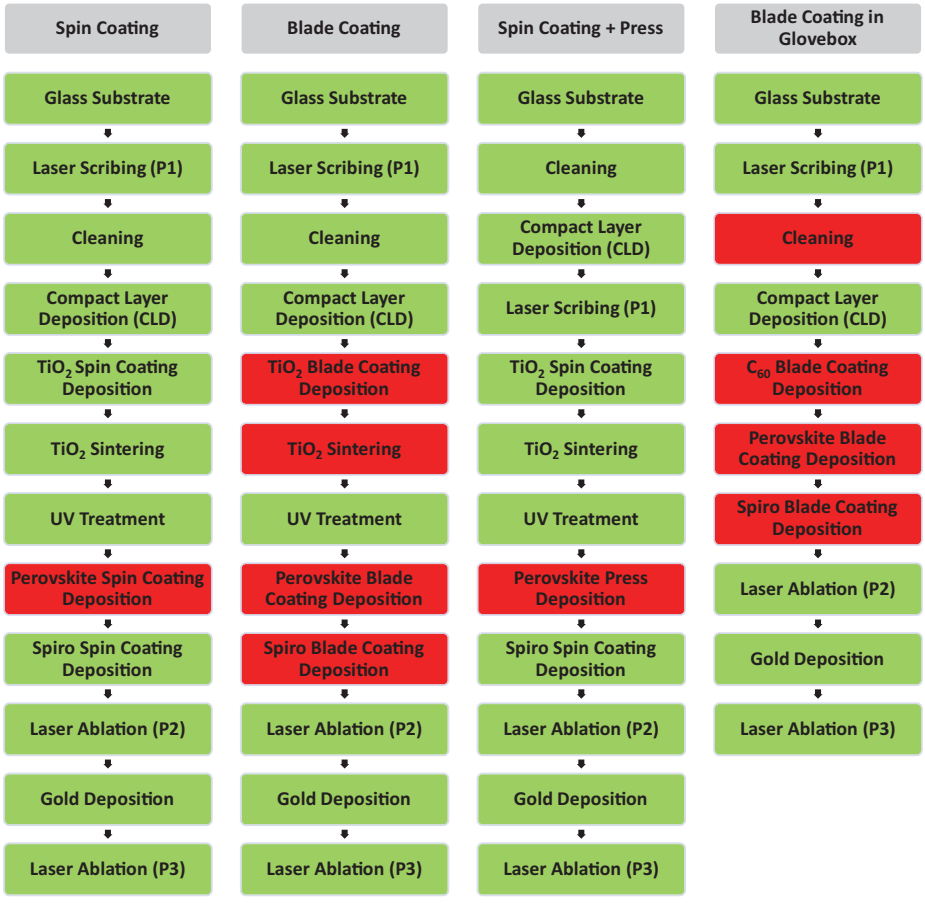

Fig. 1. Workflows of the processes Spin Coating [43], Blade Coating [43], Spin Coating + Press [44] and Blade Coating in Glovebox [45]. Steps highlighted in red are the ones characterizing each different manufacturing techniques.

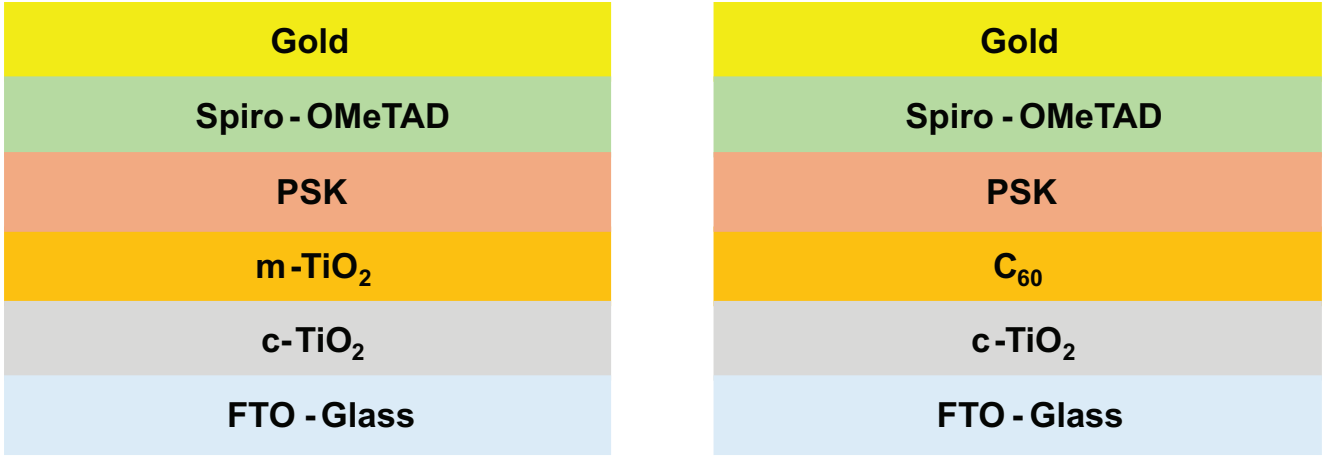

Fig. 2. Graphical representation of the minimodules. (a) Structure on the left is the one produced by Spin Coating, Blade Coating and Spin Coating + Press; (b) structure on the right is the one produced by Blade Coating in Glovebox. The only difference is the replacement of m-TiO_2 for C_{60}.

using a blade, that moves in the opposite direction of the glass at a constant velocity. PSK precursor solution is deposited first; as the blade passes over the glass, the solution is pre-dried, and then the antisolvent deposition follows. This is performed in ambient air condition.
– "Spin Coating + Press" [44]: the PSK deposition is made using the Soft-cover technique. PSK precursor solution is spread evenly onto the glass substrate applying pressure with a polyimide sheet (Kapton). Moreover, the solution comes from gas-solid reactions between PbI_2 and CH_3NH_3I with CH_3NH_2.
– "Blade Coating in Glovebox" [45]: the PSK layer deposition is made using the blade coating technique. Unlike the other blade coating process, this one is performed in a N_2 environment glovebox and comprehends a dipping in diethyl ether, the antisolvent.

3 Materials and methods

LCA is a methodology developed to evaluate and improve the environmental impact of products, processes and services. The technical references for this methodology are the ISO 14040 [46] and ISO 14044 [47], which are the international regulations describing how a LCA should be carried out. Namely, the LCA methodology follows 4 steps:
– *Goal and scope definition*: The objective of the study is defined as well as the system boundaries, the functional unit and other methodological assumptions. Pointing out the system boundaries entails the definition of all the life cycle stages and all the input and output flows that are considered in the analysis. The functional unit represents a quantifiable measure to which the results should be referred to and it should be coherent with the function of the system.
– *Life Cycle Inventory (LCI)*: In this step, all input and output fluxes of energy and matter exchanged between the environment and the product system are compiled and quantified grounding on primary data representative of the analyzed product system, integrated with secondary data derived from the literature and specific databases.
– *Life Cycle Impact Assessment (LCIA)*: This step regards the environmental impact evaluation; all the materials and energy flows identified at the LCI step are associated to environmental categories and they are converted to environmental impacts through the multiplication with specific characterization factors. Therefore, it is possible to evaluate several impact categories (such as Climate change, Ozone depletion, Particulate matter, Resource use, fossils or Resource use, minerals and metals) which depend on the selected LCIA method. The above-mentioned environmental impact categories, also called Midpoint results, can be normalized and weighted to evaluate a single score environmental impact frequently used in comparative environmental assessments.
– *Interpretation*: Results are rationalized and interpreted in order to check the consistency among the objectives stated in step 1, the LCI outlined in step 2, and the LCIA results evaluated in step 3.

3.1 Goal and scope definition

The aim of this paper is to compare the environmental performances of four different techniques to manufacture PSC mini-modules. These multi-step processes are described in Section 2 and they are named "Spin Coating", "Blade Coating", "Spin Coating + Press", and "Blade Coating in Glovebox". The cross evaluation among the four analyzed techniques is detailed by each step of the fabrication in order to identify the most critical environmental issues affecting the eco-profile of each process through a contribution analysis. The function of all the analyzed processes is fabricating a PSC mini-module. Since the sizes of the mini-modules that are compared in this study are in the range from 10 cm^2 to 64 cm^2, the functional unit is set to 1 cm^2. In order to propose a coherent comparison of all the manufacturing techniques, a single location is considered as the geographical site of mini-modules manufacturers. The selected location is Italy because the primary LCI data provider is the CHOSE, whose headquarters are set in Rome (Italy).

The LCA presented here is performed "from cradle to gate"; this definition entails that, coherently with the goal of the analysis, the study is focused on the manufacturing phase of the PV mini-modules, thus neglecting their operation phase and disposal. Figure 3 depicts a flow chart representing all life cycle stages included in the system boundaries, marked with a dashed black line.

3.2 Life Cycle Inventory (LCI)

The LCI of the PSK mini-modules fabrication techniques is based on the integration of primary data measured at the CHOSE laboratory [43], and on secondary data derived from other scientific studies and the Ecoinvent database version 3.7.1 [48], which does not include all the substances employed in the manufacturing processes, therefore ad-hoc datasets created by the authors were also used [49].

The LCI of PSK mini-modules produced by "Spin Coating" and "Blade Coating" are entirely based on onsite tests carried out at the CHOSE laboratory. All the mini-modules fabricated by CHOSE for this study have approximately the same aperture area (31.36 cm^2). More specifically, all inputs and outputs of the LCI of these mini-modules are directly based on consumptions and emissions at lab scale.

On the other hand, the LCI of the fabrication techniques "Spin Coating + Press" and "Blade Coating in Glovebox" are respectively based on the integration of the data provided by CHOSE and the information extracted from [44,45]. Therefore, the LCI of the process "Spin Coating + Press" are created through the manipulation of the "Spin Coating" inventory, whereas the inventory of the process "Blade Coating in Glovebox" grounds on the LCI of "Blade Coating". In particular, the data measured for "Spin Coating" and "Blade Coating" at laboratory scale have been used as proxies to fill the lacks in "Spin Coating + Press" and "Blade Coating in Glovebox" datasets. For instance, in order to adapt the LCI of the process "Spin Coating" to "Spin Coating + Press", the energy consumption of the pressing operation is estimated based on [44] and it is added

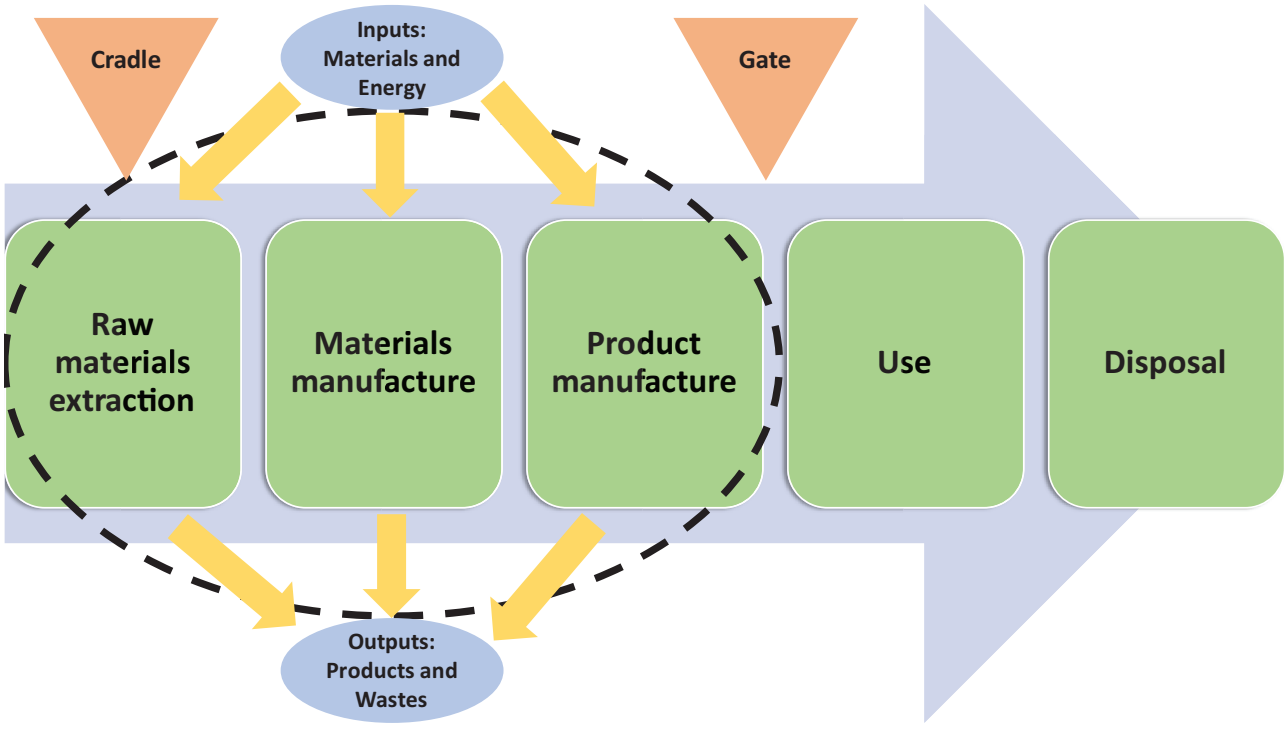

Fig. 3. System boundaries of the cradle to gate environmental assessment.

to the model. Therefore, the output of all the fabrication processes is one PSK mini-module having an aperture area equal to 31.36 cm^2. More specifically, the LCI of all steps of the production lines analysed in this paper are modelled using the following inputs:

– The amount of materials consumed.
– The energy employed.

A detailed inventory underlining differences among the production lines, in terms of consumed materials and energy, can be found in the Tables S1-S3.

3.3 Life Cycle Impact Assessment (LCIA)

Calculations are performed with the software SimaPro version 9.3.0.3. The database used is the Ecoinvent version 3.7.1. The calculation method selected for impact assessment is the EF 3.0 Method (adapted) v1.01 with EF 3.0 normalization and weighting set. The results are discussed both at Midpoint and at Endpoint level.

Midpoint environmental indicators express the LCA results with a problem-oriented logic because midpoint impact categories are associated with some environmental issues. For instance, the life cycle emissions of greenhouse gas affect the indicator "Climate Change" whereas the consumption of freshwater affects the category "Water use". These environmental indicators are calculated through the classification and characterization steps, that are mandatory according to the ISO regulations.

On the other hand, Endpoint indicators are calculated with a problem-oriented approach: normalization and weighting steps allow to sum up the environmental impact results of Midpoint categories, that can be expressed with a Single Score measured in Eco-Points (Pts). The latter approach, although not mandatory according to the ISO regulations, is frequently used to compare several product systems. In this study, the EF 3.0 normalization and weighting factors are used to calculate the single score.

4 Results and discussion

This section contains the presentation and discussion of the LCA analysis in terms of environmental impact values obtained through the Characterization and the Single Score calculation.

The manufacturing techniques analysed in this study are firstly evaluated separately (Sects. 4.1–4.4). More in detail, the results allow to evaluate the percentage burden of each manufacturing step. The results are presented focusing on those steps that are responsible for the major environmental impact contribution (pointed out by setting a 5% cut-off) and on the most representative steps on each fabrication techniques. All other steps are gathered in the "Others" voice. Moreover, for each process considered in this study, a single score is used to represent the environmental impact of each fabrication step: each column of the histogram chart that is reported in the following section represent the overall environmental burden of each manufacturing stage of the processes.

Then, Section 4.5 summarizes the comparison between the analysed processes using both Midpoint and Endpoint impact indicators.

4.1 "Spin Coating" production line

Figure 4 represents as stacked columns histograms the environmental contribution of the most important manufacturing steps of the process labelled as "Spin Coating"; each column represents a different

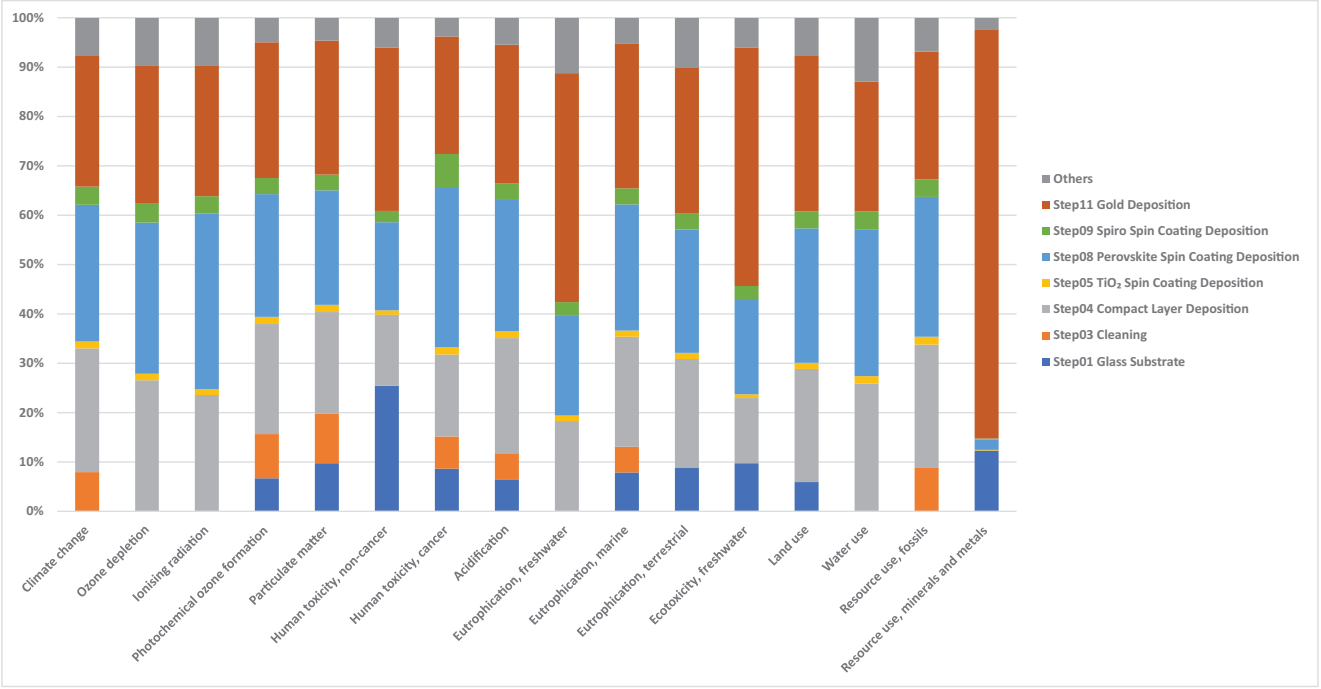

Fig. 4. Environmental impact results obtained with EF/3.0 Characterization of Spin Coating process. Detailed percentage values for each contribution can be found in the Table S4.

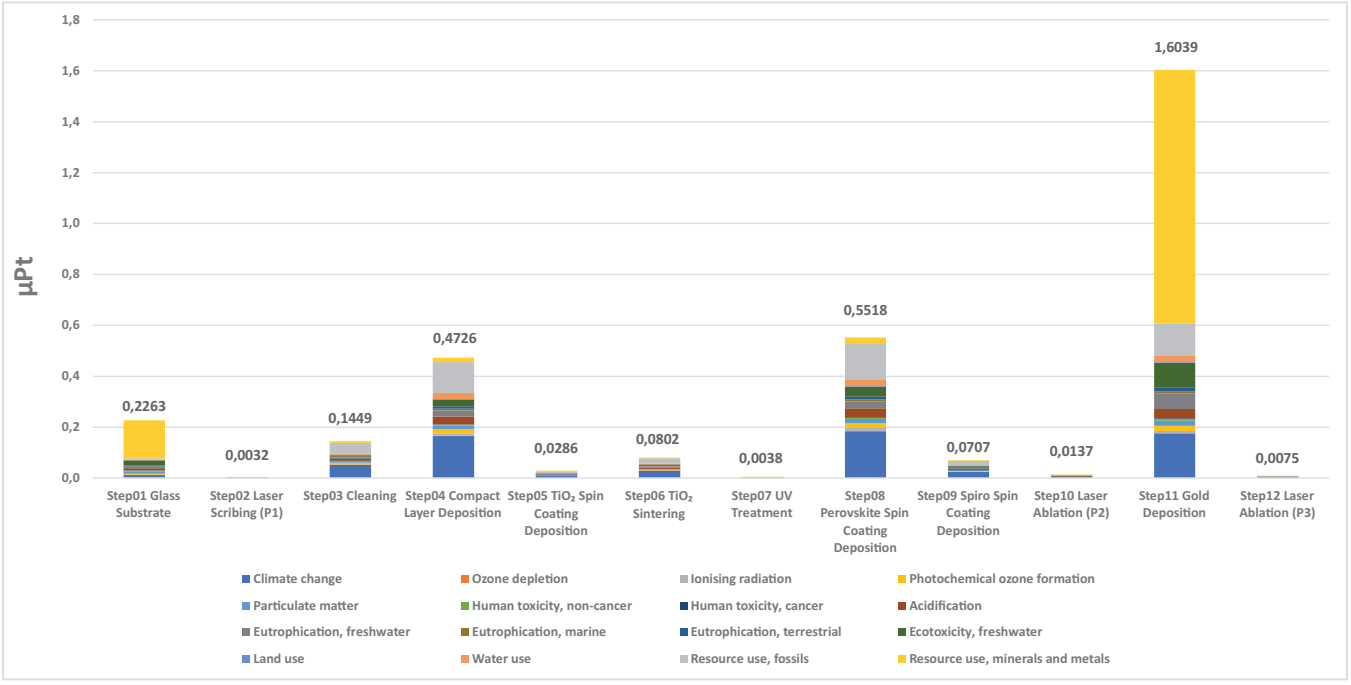

Fig. 5. Environmental impact results obtained with EF/3.0 Single Score of Spin Coating process.

environmental impact indicator proposed by the LCIA method EF3.0. A general overview of Figure 5 underlines that the most impacting steps are the glass substrate (Step 01), the c-TiO_2 deposition (Step 04), the PSK deposition (Step 08) and the gold counter electrode deposition (Step 11).

The production of the glass substrate impacts mainly in the "Human toxicity, non-cancer" and "Resource use, minerals and metals" categories for which its contribution is, respectively, 25.4% and 12.3%. Differently, for all other categories, the contribution of the glass layer is assessed below 10%. The burden of the glass layer can be almost

Table 1. Impact contributions of gold and electricity consumption in gold deposition step expressed in percentage values.

	Gold	Electricity
Climate change	8%	92%
Ozone depletion	4%	96%
Ionising radiation	10%	90%
Photochemical ozone formation	24%	76%
Particulate matter	30%	70%
Human toxicity, no-cancer	60%	40%
Human toxicity, cancer	33%	67%
Acidification	17%	83%
Eutrophication, freshwater	63%	37%
Eutrophication, marine	25%	75%
Eutrophication, terrestrial	26%	74%
Ecotoxicity, freshwater	75%	25%
Land use	26%	74%
Water use	5%	95%
Resource use, fossils	7%	93%
Resource use, minerals and metals	97%	3%

entirely attributed to the FTO-Glass production, to the soda ash consumption and to the cutting and bevelling operations. In addition, the consumption of tin remarkably affects the categories "Ecotoxicity, freshwater", "Eutrophication, freshwater" and "Resource use, minerals and metals", whereas the use of silica sand mostly affects the "Land use" indicator. Moreover, the main contribution to the impact category "Ozone depletion" is related to the aluminum oxide consumption.

Concerning the c-TiO_2 deposition step, its percentage impact is also relevant and it can be approximately estimated between 14% and 26% in all categories, except for the indicator "Resource use, minerals and metals" where it is negligible. The environmental impact of this step is mostly related to the consumption of the energy that is necessary for the deposition of c-TiO_2.

The deposition of PSK by Spin Coating represents another environmental issue for the manufacturing process analysed in this section for all the impact categories; as highlighted by the results, its contribution is assessed between 17.5% ("Human toxicity, non-cancer") and 35.7% ("Ionising radiation") and this is largely due to the electricity demanded by the deposition of this material. An exception to this consideration is represented by the category "Resource use, minerals and metals" for which the consumption of PSK determines a negligible contribution. However, the consumption of monochlorobenzene and lead determines a remarkable burden for the categories "Human toxicity, cancer", "Human toxicity, non-cancer" and "Resource use, mineral and metals" respectively.

Figure 4 highlights that the gold deposition step, necessary to produce the counter-electrode, overall represents a very critical environmental issue for the manufacturing of this solar mini-module. The environmental contribution of this stage is estimated between 23.8% ("Human toxicity, cancer") and 82.9% in "Resource use, minerals and metals". Therefore, it is possible to observe that all impact categories are strongly affected by the consumption of gold, especially those categories expressing the consumption of mineral and metals resources. However, the electricity necessary to the deposition of the golden counter-electrode also determines a relevant impact contribution for all categories. Gold plays a key role in the impact of categories "Human toxicity, no-cancer", "Eutrophication, freshwater", "Ecotoxicity, freshwater" and "Resource use, minerals and metals"; all other categories are mostly affected by the electricity consumed during the gold deposition, as summarized in Table 1.

Figure 4 underlines that the spin coating deposition of TiO_2 and Spiro, both characteristics of this process, provide a very small impact in all categories. The cleaning process also shows a limited burden that, for certain categories, achieves a percentage of 10% at max due to the use and disposal of isopropanol and acetone. The category "Others" comprehends all the steps not characteristic of the production line with a percentage burden lower than 5%. Overall, its impact contribution goes from 13.0% in the category "Water use" to 2.3% in the category "Resource use, minerals and metals".

From the single score results, represented in Figure 5, readers can observe that, considering all the above-mentioned impact categories, the total environmental burden of the "Spin Coating" production line is dominated by the gold deposition stage. Particularly, the most critical environmental indicator for this process is the "Resource use, minerals and metals". Furthermore, gold deposition is followed by the spin coating of PSK and the CLD deposition stages and by the consumption of the FTO-Glass.

4.2 "Blade Coating" production line

Concerning the "Blade Coating" process, similar considerations to the results related to the "Spin Coating" manufacturing can be done. The reason is that the two processes are almost equivalent except for the technique used for the deposition of the materials, including the PSK. According to Figure 6, the most impactful steps of the process are the use of a FTO-glass substrate, the c-TiO_2 deposition, and the gold deposition. Interestingly, the Blade Coating of PSK does not imply a very relevant environmental burden as the Spin Coating; the reason for this relevant difference is that the Blade Coating technique is less energy-intensive, due to the absence of the glovebox, and less materials-intensive than the Spin Coating. Accordingly, the percentage contribution of the PSK deposition step is assessed between 2% and 8%.

As consequence of the lower impact of the PSK deposition, the relative contribution of all the other stages, such as the Cleaning step, increases compared to the results illustrated in Figure 4. In particular, the golden counter electrode deposition turns out as the most impacting stage because its impact contributes to more than 34% of all environmental indicators. For the categories "Eutrophication, freshwater" and "Ecotoxicity, freshwater" the percentage contribution of gold deposition is around 56% and

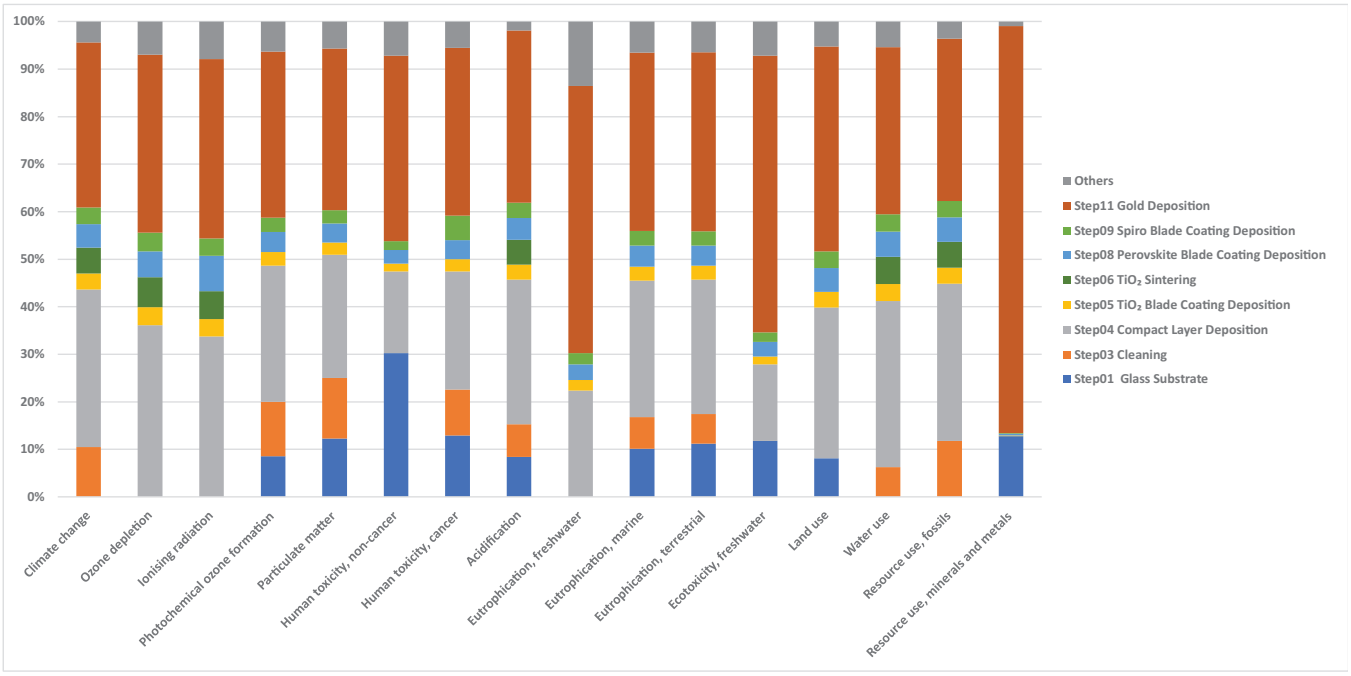

Fig. 6. Environmental impact results obtained with EF3.0 Characterization of Blade Coating process. Detailed percentage values for each contribution can be found in Table S5.

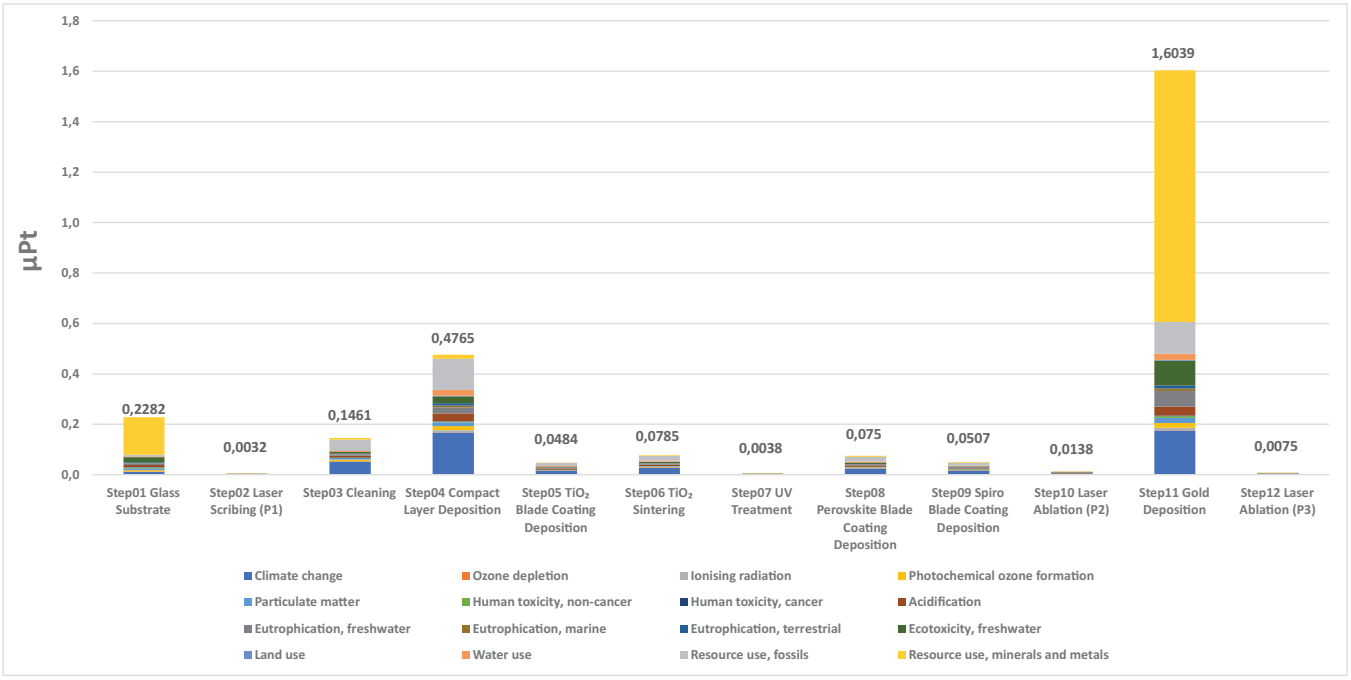

Fig. 7. Environmental impact results obtained with EF/3.0 Single Score of Blade Coating process.

58% respectively, whereas for the indicator "Resource use, minerals and metals" it is almost 84.4%. The second most impacting process of the manufacturing chain is the Compact Layer Deposition.

The Endpoint results, represented in Figure 7, are in line with the observation made in the former paragraph: the Single Score environmental burden takes into account all Midpoint impact categories and it shows that the indicator "Resource use, minerals and metals" results as the most critical one because of the gold depletion involved in the production of the counter electrode. On the other hand, the TiO_2 deposition step shows a slightly bigger value due to higher electricity consumption of the blade coater compared to the spin coater. The single score impact of the

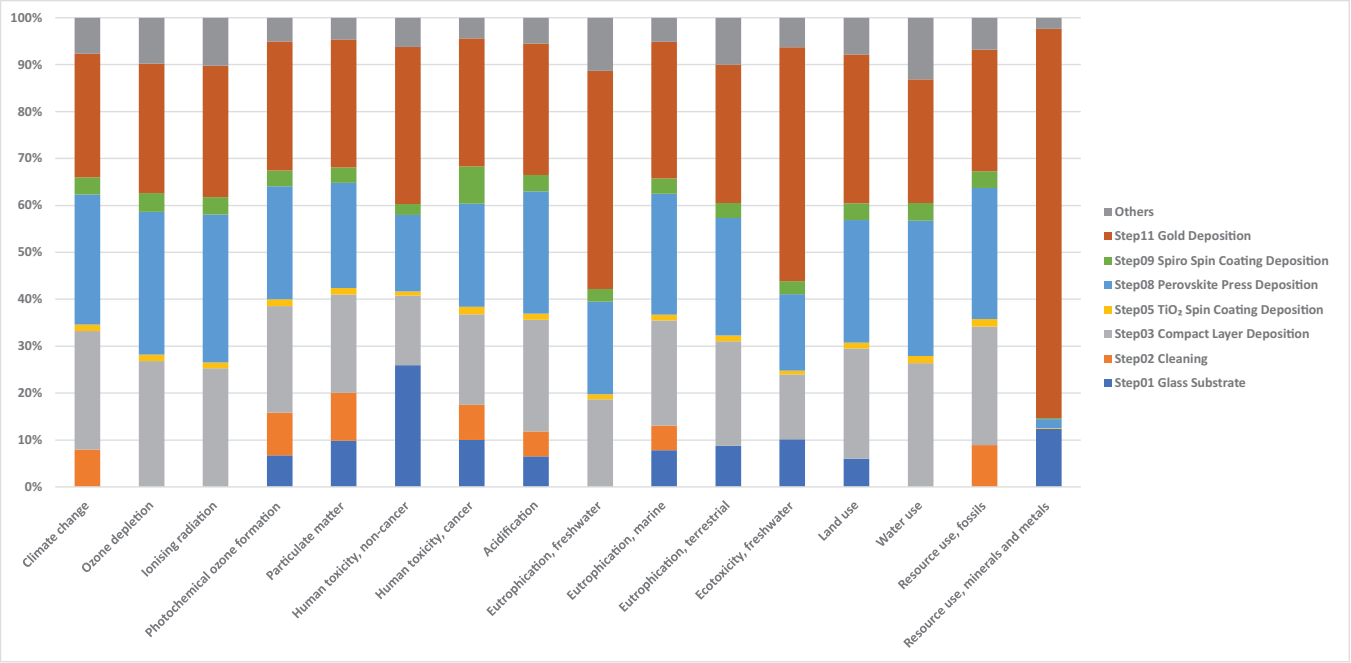

Fig. 8. Environmental impact results obtained with EF/3.0 Characterization of Spin Coating + Press process. Detailed percentage values for each contribution can be found in Table S6.

PSK deposition in this production line is strongly mitigated due to the benefits given by replacing Spin with Blade Coating.

4.3 "Spin Coating + Press" production line

The PSK solar cell manufacturing technique labelled as "Spin Coating + Press" is derived from the process called "Spin Coating": the two fabrication lines differ for the use of a press for the deposition of the PSK. According to Figure 8, the most relevant changes to the eco-profile of the product system implied by the use of the press are the mitigation of the relative impact of PSK deposition from 35.7% to 31.5% for the category "Ionising Radiation", and from 32.3% to 22.0% for the category "Human toxicity, cancer". This evidence mathematically implies bigger contributions coming from other steps of the manufacturing process. The main reasons for the impact of the PSK deposition step are related to the electricity consumption, with a partial contribution from the methylamine consumption, especially in the indicators "Human toxicity, cancer" "Ionising radiation" and "Resource use, minerals and metals". Using the press in the production line results then in a slightly lower environmental impact compared to the Spin Coating process. The main reasons for this outcome are a lower electricity consumption equal to 0.8Wh/cm^2 and the absence of any solvents (see Tabs. S1-S3).

The single score plot represented in Figure 9 underlines that, because of the employment of gold, the impact category "Resource use, minerals and metals" turns out as the most critical Midpoint indicator among those proposed by EF3.0. This outcome is similar to the one that has been obtained by analysing the "Spin Coating" process in Figure 5. More in general, the overall pattern of the eco-profile of the "Spin Coating + Press" substantially reflects that of "Spin Coating".

4.4 "Blade Coating in Glovebox" production line

Concerning the manufacturing process in which the PSK layer is deposited on the solar cell by Blade Coating in Glovebox, the PSK deposition step turns out as the most impactful fabrication step (Fig. 10). Its contribution varies as a function of the impact category from about 50% to 81.1%, except for "Resource use, minerals and metals" where it reaches 27.9% for which the gold deposition shows a dominant contribution. The additional impacts of the Blade Coating in Glovebox are mostly due to the use of diethyl ether to submerge the PSK cell that is responsible for the major environmental burdens in all indicators. Differently, the electricity demanded by the glovebox is the main contributor for the categories "Ozone depletion" and "Ionising radiation"; the use of the glovebox accounts for an electricity consumption equal to 1.3 Wh/cm^2.

As a consequence of the increasing contribution of the PSK deposition process to all impact categories, the percentage impact of the gold deposition for the counter-electrode is smaller than in the previous processes. However, its contribution is still remarkable especially for the category "Resource use, minerals and metals" where it reaches 60.3% and both the depletion of gold and the consumption of electricity are responsible for such high percentage value.

Concerning the other steps of the process, the Cleaning phase and the Spiro deposition step also show minimal contributions while the tin consumption in FTO-glass has a relevant impact only in three categories: "Human toxicity,

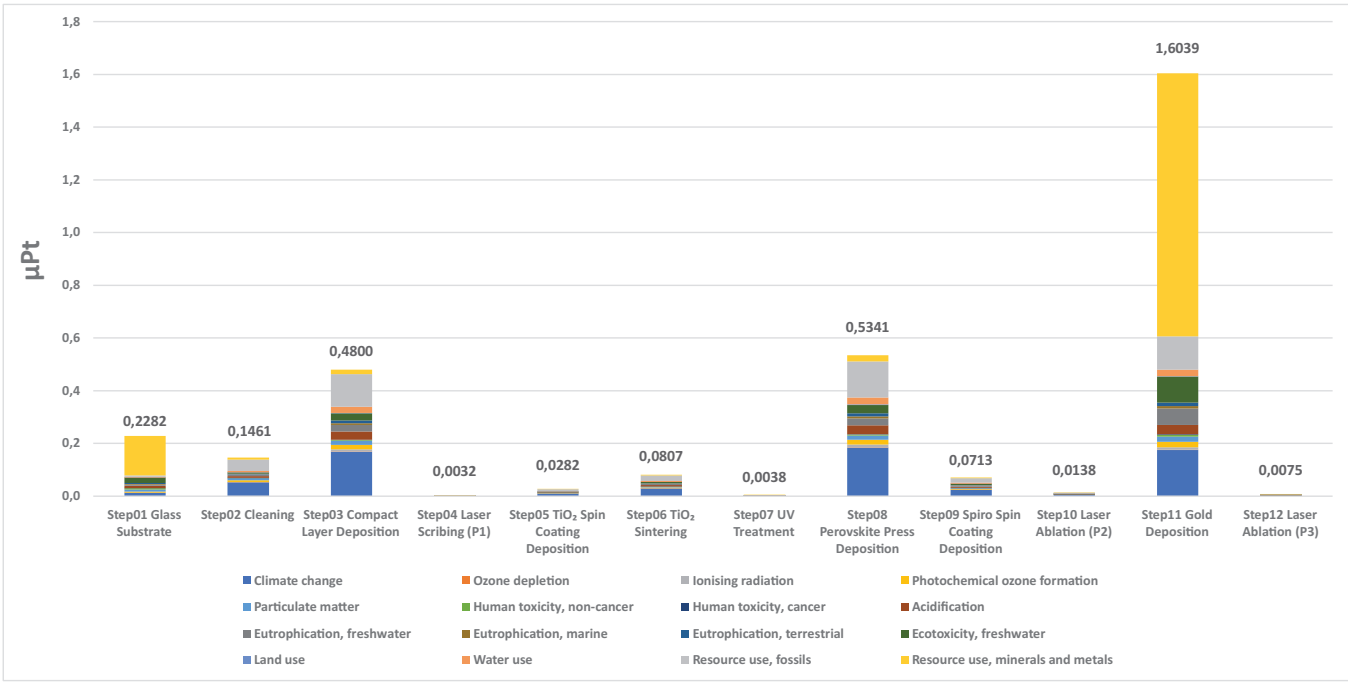

Fig. 9. Environmental impact results obtained with EF/3.0 Single Score of Spin Coating + Press process.

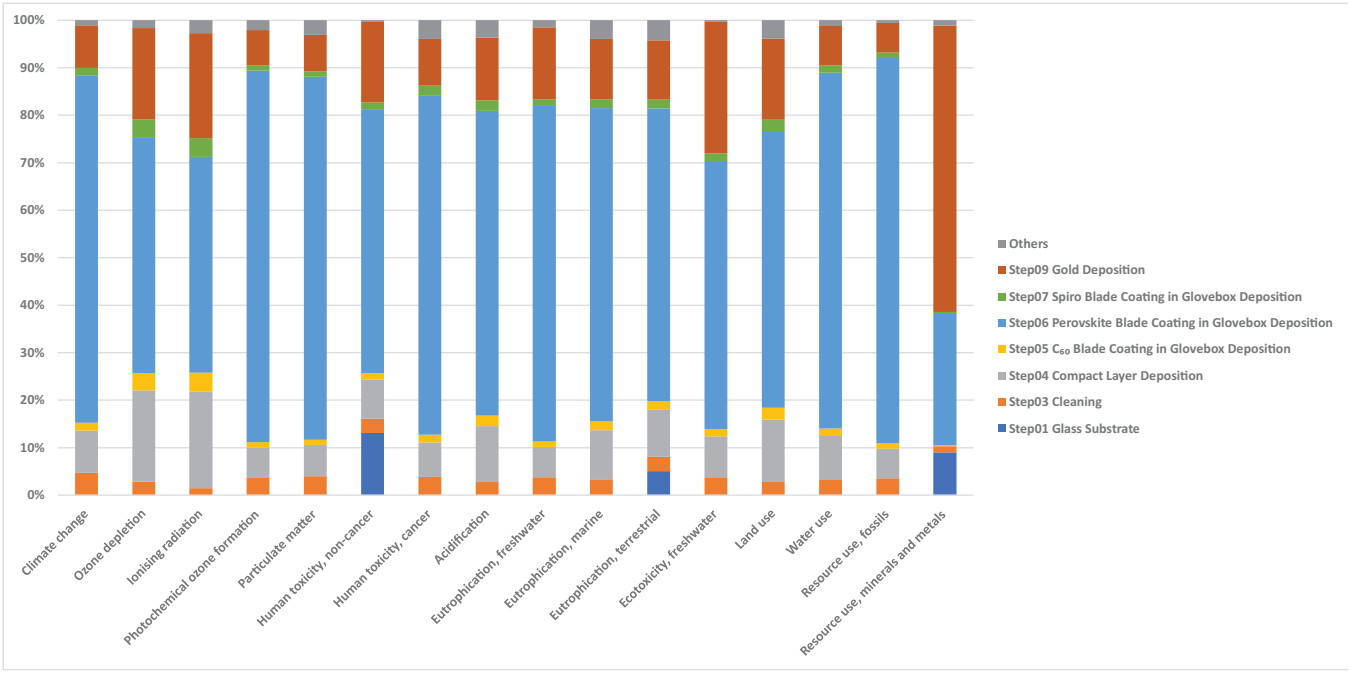

Fig. 10. Environmental impact results obtained with EF/3.0 Characterization of Blade Coating in Glovebox process. Detailed percentage values for each contribution can be found in Table S7.

non-cancer", "Eutrophication, terrestrial" and "Resource use, minerals and metals" where it reaches 13.1%, 5.3% and 9.0% respectively.

Also, the CLD step shows relevant impact contribution because of the 1-butanol consumption and the electricity demanded by the process.

Figure 11 represents the single score results relative to the manufacturing steps; it can be observed that, coherently with the results expressed at midpoint level, the most impactful step is the one related to the PSK deposition. According to the outputs returned by the LCA model, the most critical indicators that contribute to the burden of the deposition of the PSK layer are "Climate change", "Resource use, fossils" and "Resource use, minerals and metals". Also, similarly to the solar cells manufacturing techniques analyzed in the former paragraphs, the gold deposition is a strongly impacting process.

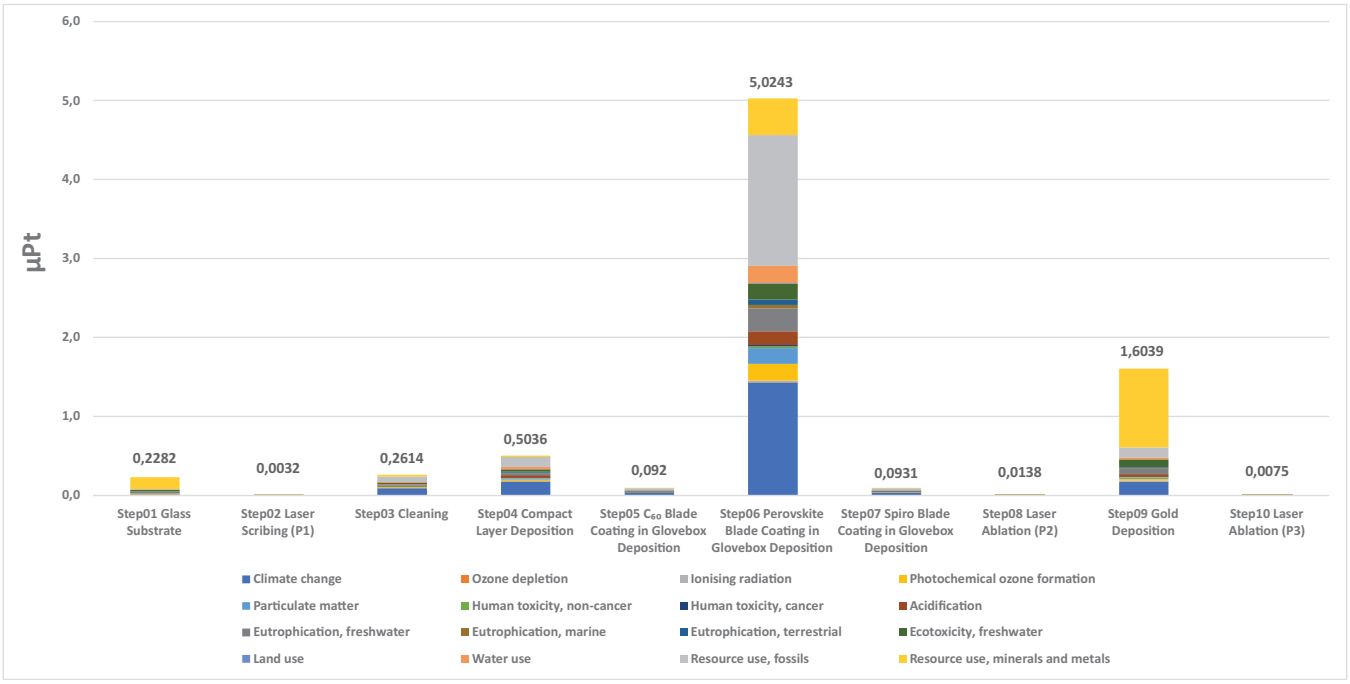

Fig. 11. Environmental impact results obtained with EF/3.0 Single Score of Blade Coating in Glovebox process.

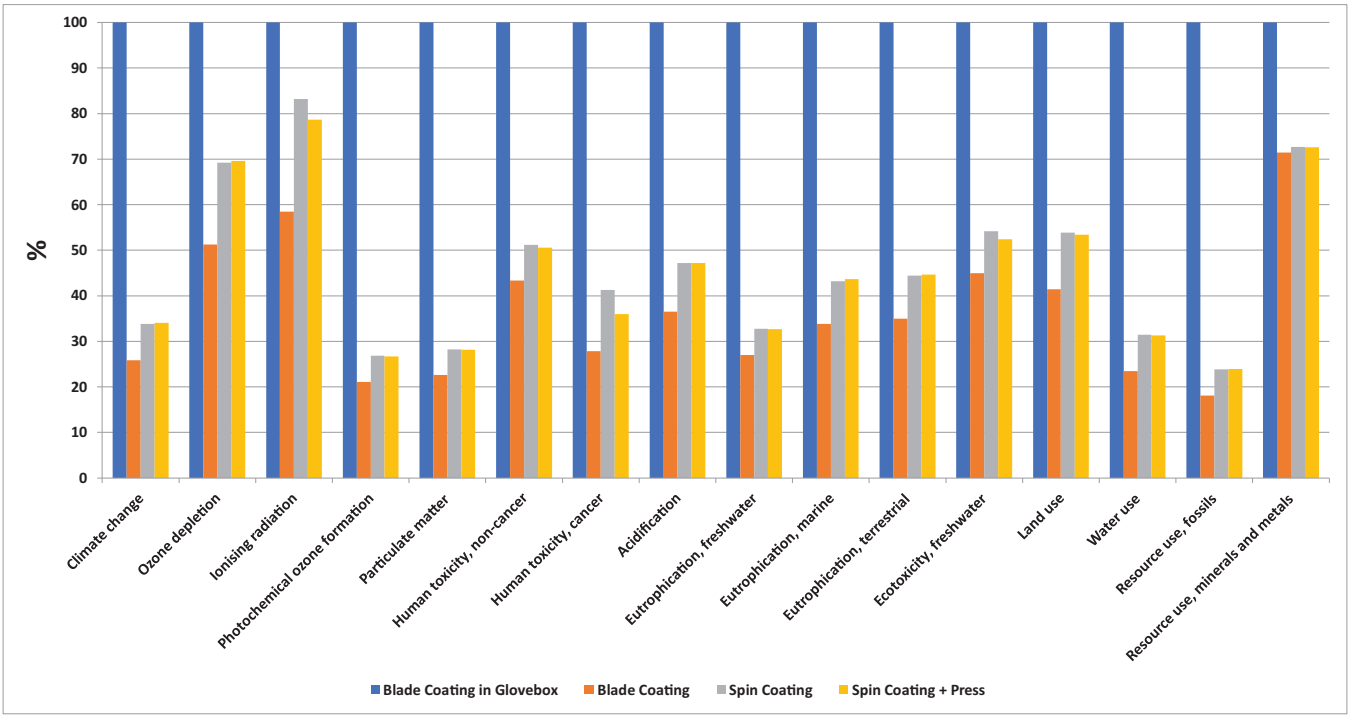

Fig. 12. Environmental impact results obtained with EF/3.0 Characterization of comparison between all processes. Detailed percentage values for each indicator can be found in Table S8.

4.5 Comparative LCA results

The former paragraphs describe separately the eco-profile of all production lines for the fabrication of PSK solar cells. In this subsection, a global comparison of all the manufacturing solution considered in this study is presented as midpoint environmental indicators and as single score results. Figure 12 represents a histogram chart in which the environmental indicators of each process are represented as relative results compared to the most impacting manufacturing technique whose burden value is set to 100%.

From the environmental characterization results, represented in Figure 12, it can be observed that the process "Blade Coating in Glovebox" turns out as the most impacting for all the environmental impact categories. Such evidence is motivated by the high environmental burden of the PSK deposition stage, whose environmental sustainability is negatively affected by the consumption of diethyl ether and the electricity consumption of the glovebox. As underlined in Figure 12, the environmental impacts of the other manufacturing processes is considerably lower than the process "Blade Coating in Glovebox", especially the categories "Resource use, fossils", "Photochemical ozone formation", "Particulate matter" and "Climate change", for which the LCA results of the other manufacturing processes are approximately between 18% and 34% compared to the impact of the process "Blade Coating in Glovebox".

Concerning the process "Spin Coating" and "Spin Coating + Press", the results shows that their eco-profiles are very similar; the most remarkable differences between these two processes are related to the indicators "Ionising radiation", "Human Toxicity, cancer", "Ecotoxicity, freshwater" and "Land use". In particular, a general overview of the midpoint results shows that the process "Spin Coating + Press" is slightly less impacting than "Spin Coating". The results demonstrate that, although the use of a press requires the consumption of energy, which is lower than the amount required by the usage of the spin coater in glovebox, overall it allows to mitigate the consumption of solvents, such as dimethyl sulfoxide and monochlorobenzene.

According to the results, the least impactful solar cells production route turns out to be the "Blade Coating". The impact of the mini-modules produced with this technique are $5\% - 10\%$ lower than the spin coated devices in almost all categories; for certain indicators, such as "Ozone depletion" and "Ionising radiation", this percentage achieves 20%. This is because blade coating overall implies the lowest consumption of electricity and materials; in addition, also the use of more environmentally friendly solvents, like isopropanol instead of monochlorobenzene, results to be effective to improve the eco-profile of the final product. Concerning the category "Resource use, minerals and metals", the environmental performance of the processes "Spin Coating", "Blade Coating" and "Spin Coating + Press" are very close; this is due to the elevated impact of gold deposition step that dominates this category and that is equal for all processes. All midpoint impact categories for all the manufacturing techniques are available in Table 2.

In the previous paragraphs, four different manufacturing processes are cross-evaluated as function of the LCA impact category. However, in order to compare the abovementioned processes using a single indicator summarizing all Midpoint impact indicators, their single score is represented in the histogram illustrated in Figure 13. This Figure demonstrates that, coherently with the interpretation of the LCA characterization, the "Blade Coating in Glovebox" process exhibit a very high Pt value, as the impact value results to be more than doubled in respect to the other 3 processes. This is because for this process, both the PSK and the gold deposition represent critical environmental issues, the former for the categories "Climate change" and "Resource use, fossils", and the latter for "Resource use, minerals and metals". Among the other fabrication processes, the differences in terms of single score are not strongly remarked. For all of them, the previous sections underline that the most critical manufacturing step is the gold deposition, which is equivalent in all the fabrication processes compared in this study. However, "Blade Coating" turns out as the less impactful manufacturing technique since blade coating PSK deposition allows for a considerable mitigation of the "Climate change" compared to the solutions based on spin coating, whose single score impacts result to be approximately equivalent.

The previous section underline that the most critical manufacturing step is the gold deposition, which is equivalent in all the fabrication processes compared in this study. For this reason, gold replacement is a game changer in the PSC fabrication also from the environmental point of view independently from the PVK deposition technique. In the last years many efforts were focused on the research for gold-alternatives and low carbon-footprint materials. The most important emerging materials for single junction PVK photovoltaics are certainly carbon-based electrodes [49–51]. Carbon electrodes are generally made from a mixture of carbon black and graphite which are embedded in an organic binder [52]. In this way the carbon paste or ink can be processed through vacuum-free and ambient air scalable techniques (blade coating, hot press, lamination) [53–56]. Moreover, carbon electrode is thermally and chemically stable, naturally hydrophobic and has intrinsic p-type behavior which is useful for HTM-free devices [52,57,58]. Depending on the binder used, it can be processed at low temperature ($<120\,°C$) with a competitive efficiency of 20% on small area device [59]. Other new routes are in continuous exploration, also with remarkable results, such as solution-processed electrode based on nickel-bismuth alloy presented by Li et al. with an exceptional efficiency of 21% [60] or carbon nanotubes composites with Poly(methyl Methacrylate) (PMMA) or Polycarbonate (PC), materials that mixed together can provide electrical connection and a proper encapsulation of the device [61].

4.6 Discussion

From the results reported in the previous section, it can be deduced that the Blade Coating technique is the least impactful. This evidence is mostly due to (i) a minor electricity consumption, resulting from the absence of the glovebox, (ii) a higher efficiency in the use of materials, and (iii) the usage of less harmful substances, like isopropanol instead of monochlorobenzene.

Spin Coating and Spin Coating + Press techniques have very similar eco-profiles; they only differ in the PSK deposition step. The Spin Coating process' eco-profile is determined by the presence of more toxic substances, like monochlorobenzene, DMSO, DMF and various lead compounds. On the other hand, Spin Coating + Press, although consuming fewer toxic materials, is characterized by a strong deployment of methylamine to produce the PSK precursor solution.

Table 2. Environmental impact in absolute value for all processes in all impact categories.

	Spin Coating	Blade Coating	Spin Coating + Press	Blade Coating in Glovebox	Unit
Climate change	2.54×10^{-2}	1.94×10^{-2}	2.56×10^{-2}	7.52×10^{-2}	kg CO_2 eq
Ozone depletion	3.12×10^{-9}	2.31×10^{-9}	3.14×10^{-9}	4.51×10^{-9}	kg CFC11 eq
Ionising radiation	3.03×10^{-3}	2.13×10^{-3}	2.87×10^{-3}	3.65×10^{-3}	kBq U-23 eq
Photochemical ozone formation	6.18×10^{-5}	4.86×10^{-5}	6.16×10^{-5}	2.31×10^{-4}	kg NMVOC eq
Particulate matter	4.93×10^{-10}	3.94×10^{-10}	4.92×10^{-10}	1.75×10^{-9}	disease inc.
Human toxicity, non-cancer	2.26×10^{-10}	1.91×10^{-10}	2.23×10^{-10}	4.41×10^{-10}	CTUh
Human toxicity, cancer	8.40×10^{-12}	5.67×10^{-12}	7.33×10^{-12}	2.04×10^{-11}	CTUh
Acidification	1.15×10^{-4}	8.92×10^{-5}	1.15×10^{-4}	2.44×10^{-4}	mol H^+ eq
Eutrophication, freshwater	7.70×10^{-6}	6.35×10^{-6}	7.68×10^{-6}	2.35×10^{-5}	kg P eq
Eutrophication, marine	1.93×10^{-5}	1.51×10^{-5}	1.94×10^{-5}	4.45×10^{-5}	kg N eq
Eutrophication, terrestrial	2.15×10^{-4}	1.69×10^{-4}	2.16×10^{-4}	4.84×10^{-4}	mol N eq
Ecotoxicity, freshwater	4.53×10^{-1}	3.76×10^{-1}	4.38×10^{-1}	8.36×10^{-1}	CTUe
Land use	6.87×10^{-2}	5.28×10^{-2}	6.81×10^{-2}	1.27×10^{-1}	Pt
Water use	1.24×10^{-2}	9.27×10^{-3}	1.24×10^{-2}	3.95×10^{-2}	m^3 depriv.
Resource use, fossils	3.81×10^{-1}	2.89×10^{-1}	3.82×10^{-1}	1.60	MJ
Resource use, minerals and metals	1.01×10^{-6}	9.97×10^{-7}	1.01×10^{-6}	1.40×10^{-6}	kg Sb eq

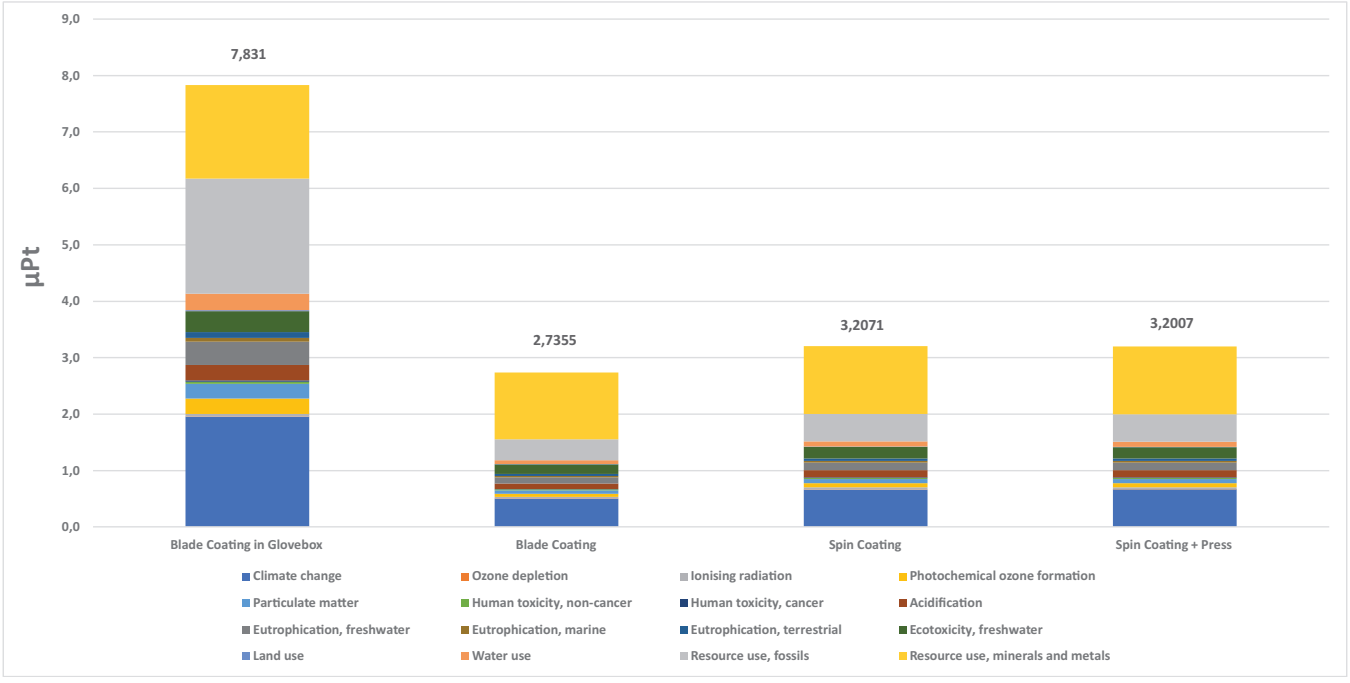

Fig. 13. Environmental impact results obtained with EF/3.0 Single Score of comparison between all processes.

Moreover, the soft cover deposition entails the use of a Kapton sheet, which is not clear from the literature [44] if can be reused or not. The use of a spin coater in glovebox results in a slightly increase of electricity consumption compared to the use of a press, going from 1.1 Wh/cm^2 to 1.9 Wh/cm^2.

Blade Coating in Glovebox process turns out to be the least environmentally friendly, mainly due to the high consumption of diethyl ether, which is absent in the other processes. Furthermore, such technique uses toxic solvents, like monochlorobenzene and THF, even in the ETL deposition step. From the energy requirement perspective,

the use of the glovebox in every deposition step entails the consumption of more electricity compared to the other process.

Concerning the critical issue of using lead in PSC production, many studies show the possibility of lead sequestration in PVK devices by functionalization of the encapsulant material and sustainable pathway for recycling lead from dead devices [62–65]. Indeed, identifying and consolidating lead sequestration and recycling strategies would be potentially very important for future PSC development [66]. Materials with Pb-sequestering properties can be thiol-functionalized nanoparticles or porous polymer-metal organic framework (MOF) composite material [65] or multifunctional mesoporous amino-grafted-carbon net [68]. In another concept [69], hydroxyapatite nanoparticles (HAP NPs) are blended with TiO_2 NPs to prepare mixed mesoporous scaffolds which are used to prepare high efficiency PSC and to limit the Pb-concentration in water. Lead-absorbing film (e.g. MOF or P,P';-di(2-ethylhexyl)methanediphosphonic acid − DMDP) can be deposited on the glass side of the front transparent conductive electrode and on the back electrode side [70]. We envision that the Pb-sequestering materials eventually will make PSC safe for the environment, thus becoming a necessary component in the device fabrication chain.

The construction process of a single-Si photovoltaic cell turns out to have an environmental footprint very close to those of Spin Coating and Spin Coating + Press techniques, although the former is slightly lower. Nevertheless, the Blade Coating and Blade Coating in Glovebox technique remain respectively the least and most impactful among the five. Single score values calculated for this comparison can be found in Table 3, while a deeper inspection concerning the comparison accounting for the manufacturing of a single-Si photovoltaic cell can be found in Figures S1–S3.

4.7 Sensitivity analysis

A sensitivity analysis of the studied techniques has been conducted by comparing 3 scenarios differing for the electricity mix compositions. Among all the main contributors to the environmental profile that could be selected for the sensitivity analysis, we chose to focus on the Italian electricity mix because energy production pathways are expected to rapidly change in parallel with the sustainable energy transition [71,72].

The proposed scenarios have been built as follows:

- Scenario 1: baseline scenario in which the electricity comes from the current Italian energy mix, dominated by natural gas [48].
- Scenario 2: future scenario foreseeing the evolution of the Italian energy mix in 2030 according to current policies (BASE). In this scenario, a higher penetration of renewable energy sources is expected. This includes an increase in the share of hydropower from 10% to over 15%; the contributions of wind and solar power will rise respectively from 5% to 7.5% and from 7% to almost 10% [71,72].
- Scenario 3: future scenario foreseeing the evolution of the Italian energy mix in 2030 according to the "Integrated National Energy and Climate Plan" (INECP) [71,72]. According to the INECP projections, a complete phase-out of coal is planned while the share of solar power in the national electricity mix is expected to exceed 20%.

Accordingly, the contribution of renewable energy sources to the Italian electricity mix increases from Scenario 1 to Scenario 3.

Table 3. Environmental impact results obtained with EF/3.0 Single Score of comparison between the four manufacturing techniques and mainstream single-Si photovoltaic cell.

	$\mu Pt/cm^2$
Blade Coating in Glovebox	7.8310
Blade Coating	2.7355
Spin Coating	3.2071
Spin Coating + Press	3.2007
Single-Si Cell	3.1428

Single score results of the four production lines are presented in Figure 14. Remarkably, the ranking among the manufacturing techniques is not affected by the electricity mix, and Blade Coating results as the most environmentally sustainable solution in all scenarios. However, a slight environmental impact mitigation can be observed for all the techniques due to the increasing contribution of renewable energy sources. As expected, the most impactful scenario is the one based on the current Italian energy mix and scenario 3 presents the lowest environmental impact. Nevertheless, the single score results among different scenarios are very similar, presenting only very small differences. Spin Coating and Spin Coating + Press are the most influenced techniques by the change in the electricity mix, reducing their impact by about 21%. Blade Coating is less affected, lowering its impact by about 17% while Blade Coating in Glovebox can benefit from an 8% decrease. These results entail that the electricity consumption has major importance for the eco-profile of Spin Coating and Spin Coating + Press, slightly less for Blade Coating and it affects the Blade Coating in Glovebox only for 8%. These results can be explained considering that the Blade Coating technique is less energy intensive than the competitors, while for the Blade Coating in Glovebox a major contribution comes also from the use of diethyl ether. It is important also to notice that, changing the electricity scenarios, the overall impact of Spin Coating and Spin Coating + Press tends to be the same.

Process contributors to the overall impact of the technologies do not vary for all impact categories regardless of the selected scenarios, except for the burden of electricity consumption that decreases when moving towards a transition to renewable sources.

More extensive results can be found in Figures S4–S7.

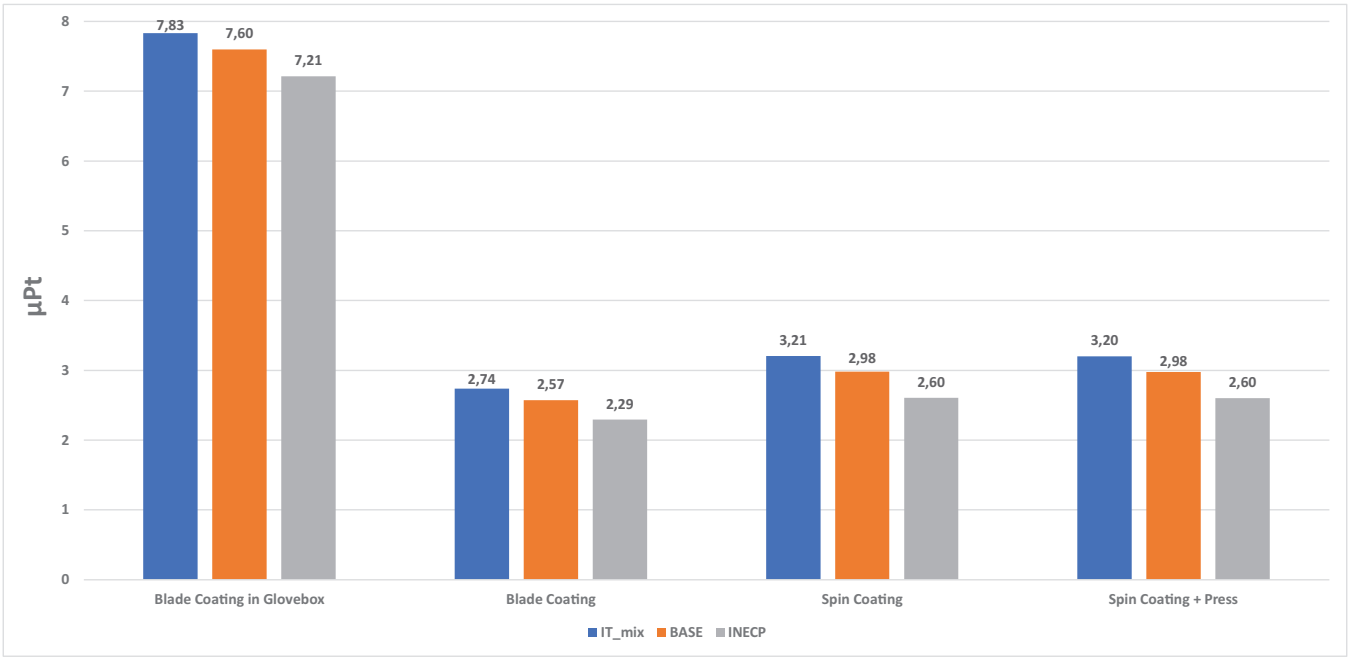

Fig. 14. Environmental impact results obtained with EF/3.0 Single Score of comparison between all processes among the three scenarios.

5 Conclusions

This study addresses the comparison among 4 manufacturing processes of PSK solar mini-modules. These fabrication processes are composed of several steps, but the main difference among them is the deposition method of PSK material that can be accomplished through Spin Coating, Blade Coating, Spin Coating assisted by a Press, and Blade Coating in Glovebox environment. However, some minor differences can be observed along with the whole production chain of the mini-modules.

A consistent LCA model is developed to cross-evaluate the environmental performances of all these fabrication techniques by focusing on several environmental indicators proposed by the LCIA method EF3.0 and on a single score.

Among the four manufacturing lines, the most environmentally sustainable is the Blade Coating, featuring as the most optimized process, since it consumes less energy and toxic substances. Spin Coating and Spin Coating + Press present little differences from an environmental impact point of view, underlining that there is no difference between the Spin Coating and the Soft Cover perovskite deposition. Blade Coating in Glovebox results as the most impactful techniques, due to both energy-intensive production steps, and the large use of toxic solvents. It must be considered that results are strongly affected by electricity and gold consumptions, thus making the gathering of very accurate data essential.

As a limitation of this study, it should be noted that these results are valid only for lab scale $\approx 30 cm^2$ and calculations might lead to quite different conclusions if scale up is considered. Then, further studies can be focused on a prospective LCA analysis aimed to assess the future environmental impacts of PSK production processes when they will reach an industrial scale manufacturing level, and PSCs will be more technologically mature. Moreover, the system boundaries could also be extended beyond the cradle-to-gate level to include the operation and end of life stages of mini-modules.

List of abbreviations

GHG	Greenhouse Gas
PV	Photovoltaic
LCA	Life Cycle Assessment
PSC	Perovskite Solar Cell
PSK	Perovskite
TCO	Transparent Conductive Oxide
HTL	Hole Transporting Layer
ETL	Electron Transporting Layer
CVD	Chemical Vapour Deposition
HCVD	Hybrid Chemical Vapour Deposition
CHOSE	Center for Hybrid and Organic Solar Energy
LCI	Life Cycle Inventory
LCIA	Life Cycle Impact Assessment
CLD	Compact Layer Deposition
OSC	Organic Solar Cell
PMMA	Poly(methyl Methacrylate)
PC	Polycarbonate
INECP	Integrated National Energy and Climate Plan

Acknowledgments

Authors thank Dr. Lorenzo Zani, Institute of Chemistry of Organometallic Compounds at Consiglio Nazionale delle Ricerche, for helping in estimating the volume of perovskite precursor solution used in the manufacturing technique Spin Coating + Press. Luigi Vesce and Maurizio Stefanelli would like to thank Prof. Aldo Di Carlo, University of Rome Tor Vergata, for fruitful and inspiring discussions.

Funding

This research was funded by the European Union's Horizon Europe programme, through a FET Proactive research and innovation action under grant agreement No. 101084124 (DIAMOND).

Conflicts of interest

The authors declare no conflicts of interest.

Data availability statement

The original contributions presented in the study are included in the article/supplementary material, further inquiries can be directed to the corresponding authors.

Author contribution statement

Conceptualization: A.S., L.V., M.L.P – Methodology: A.S., L.V., M.L.P – Validation: M.L.P. – Formal analysis: F.R., L.R., M.S. – Investigation: F.R., L.R., M.S. – Resources: L.V. – Data Curation: F.R., L.R. –Writing – Original Draft: F.R., L.R., M.S. – Writing – Review & Editing: A.S., L. V., M.L.P –Visualization: F.R., L.R., M.S., L.V., M.L.P. – Supervision: L.V., M.L.P. All authors reviewed the results and approved the final version of the manuscript.

Supplementary material

Supporting Information provided by the Authors. The Supplementary Material is available at https://epj-pv.org/10.1051/epjpv/2024014/olm.

References

1. Paris Agreement on climate change. https://www.consilium.europa.eu/en/policies/climate-change/paris-agreement/
2. European: Green Deal. https://www.consilium.europa.eu/en/policies/green-deal/
3. Fit for 55. https://www.consilium.europa.eu/en/policies/green-deal/fit-for-55-the-eu-plan-for-a-green-transition/
4. Agenda 2030 – sustainable development goals. https://sdgs.un.org/2030agenda
5. IPCC, AR6 Synthesis Report: Climate Change 2023 (2023). https://www.ipcc.ch/report/sixth-assessment-report-cycle/
6. International Renewable Energy Agency Abu Dhabi, *Global energy transformation; A roadmap to 2050* (IRENA, 2019)
7. International Renewable Energy Agency Abu Dhabi, *World energy transitions outlook 2023 1.5° c pathway preview* (IRENA, 2023). https://www.irena.org/Publications/2023/Mar/World-Energy-Transitions-Outlook-2023
8. S. Pescetelli et al., Integration of two-dimensional materials-based perovskite solar panels into a stand-alone solar farm, Nat. Energy **7**, 597 (2022). https://doi.org/10.1038/s41560-022-01035-4
9. M.L. Parisi, A. Sinicropi, Closing the loop for perovskite solar modules, Nat. Sustain. **4**, 754 (2021). https://doi.org/10.1038/s41893-021-00735-1
10. IEA, Electricity mix in China, January-November 2020, IEA. https://www.iea.org/data-and-statistics/charts/electricity-mix-in-china-january-november-2020
11. IEA, Solar PV manufacturing capacity by country and region, 2021, IEA. https://www.iea.org/data-and-statistics/charts/solar-pv-manufacturing-capacity-by-country-and-region-2021
12. K.P. Goetz, A.D. Taylor, Y.J. Hofstetter, Y. Vaynzof, Sustainability in perovskite solar cells, ACS Appl. Mater. Interfaces **13**, 1 (2021). https://doi.org/10.1021/acsami.0c17269
13. V. Fthenakis, P.A. Lynn, *Electricity from Sunlight: Photovoltaic-Systems Integration and Sustainability*, 2nd edn. (Wiley, 2018)
14. M. A. Green et al., Solar cell efficiency tables (version 62), Prog. Photovolt.: Res. Appl. **31**, 651 (2023). https://doi.org/10.1002/pip.3726
15. A. Reinders, P. Verlinden, W. van Sark, A. Freundlich, *Photovoltaic Solar Energy: From Fundamentals to Applications* (John Wiley & Sons, 2017)
16. S.J. Fonash, *Solar Cell Device Physics*, 2nd edn. (Elsevier, 2010)
17. H.J. Snaith, Present status and future prospects of perovskite photovoltaics, Nat. Mater. **17**, 372 (2018). https://doi.org/10.1038/s41563-018-0071-z
18. S.-P. Feng et al., Roadmap on commercialization of metal halide perovskite photovoltaics, J. Phys. Mater. **6**, 032501 (2023). https://doi.org/10.1088/2515-7639/acc893
19. NREL Best Research-Cell Efficiency Chart. https://www.nrel.gov/pv/cell-efficiency.html
20. G. Giuliano, A. Bonasera, G. Arrabito, B. Pignataro, Semitransparent perovskite solar cells for building integration and tandem photovoltaics: design strategies and challenges, Solar RRL **5**, 2100702 (2021). https://doi.org/10.1002/solr.202100702
21. D. B. Ritzer et al., Translucent perovskite photovoltaics for building integration, Energy Environ. Sci. **16**, 2212 (2023). https://doi.org/10.1039/d2ee04137e
22. A.S.R. Bati, Y.L. Zhong, P.L. Burn, M.K. Nazeeruddin, P.E. Shaw, M. Batmunkh, Next-generation applications for integrated perovskite solar cells, Commun. Mater. **4**, 2 (2023). https://doi.org/10.1038/s43246-022-00325-4
23. J.Y. Kim, J.W. Lee, H.S. Jung, H. Shin, N.G. Park, High-efficiency perovskite solar cells, Chem. Rev. **120**, 7867 (2020). https://doi.org/10.1021/acs.chemrev.0c00107
24. M. Stefanelli, L. Vesce, A. Di Carlo, Upscaling of carbon-based perovskite solar module, Nanomaterials **13**, 313 (2023). https://doi.org/10.3390/nano13020313
25. D. Zhou, T. Zhou, Y. Tian, X. Zhu, Y. Tu, Perovskite-based solar cells: materials, methods, and future perspectives, J. Nanomater. **2018**, 1 (2018). https://doi.org/10.1155/2018/8148072
26. D.K. Lee, N.G. Park, Materials and methods for high-efficiency perovskite solar modules, Solar RRL **6**, 2100455 (2022). https://doi.org/10.1002/solr.202100455
27. A. Ummadisingu, M. Grätzel, Revealing the detailed path of sequential deposition for metal halide perovskite formation, Sci. Adv., **4**, 2 (2018). https://www.science.org/doi/10.1126/sciadv.1701402
28. D. Li et al., A review on scaling up perovskite solar cells, Adv. Funct. Mater. **31**, 2008621 (2021). https://doi.org/10.1002/adfm.202008621
29. H.-J. Kim, H.-S. Kim, N.-G. Park, Progress of perovskite solar modules, Adv. Energy Sustain. Res. **2**, 2000051 (2021). https://doi.org/10.1002/aesr.202000051
30. S.F. Ahmed et al., Perovskite solar cells: thermal and chemical stability improvement, and economic analysis, Mater. Today Chem. **27**, 101284 (2023). https://doi.org/10.1016/j.mtchem.2022.101284
31. Z. Yang, C.C. Chueh, F. Zuo, J.H. Kim, P.W. Liang, A.K.Y. Jen, High-performance fully printable perovskite solar cells via blade-coating technique under the ambient condition, Adv. Energy Mater. **5**, 1500328 (2015), https://doi.org/10.1002/aenm.201500328
32. S.G. Motti et al., Controlling competing photochemical reactions stabilizes perovskite solar cells, Nat. Photonics **13**, 532 (2019). https://doi.org/10.1038/s41566-019-0435-1
33. L. Vesce et al., Scaling-up of Dye Sensitized Solar Modules (2018). http://www.chose.uniroma2.it/ricerca/pubblicazioni/342-scaling-up-of-dye-sensitized-solar-modules.html
34. L. Vesce et al., Hysteresis-free planar perovskite solar module with 19.1% efficiency by interfacial defects passivation, Solar RRL **6**, 2101095 (2022). https://doi.org/10.1002/solr.202101095
35. R. Frischknecht, Methodology Guidelines on Life Cycle Assessment of Photovoltaic Task 12 PV Sustainability. https://iea-pvps.org/wp-content/uploads/2020/07/IEA_Task12_LCA_Guidelines.pdf
36. A. Wade, P. Stolz, R. Frischknecht, G. Heath, P. Sinha, The product environmental footprint (PEF) of photovoltaic modules—Lessons learned from the environmental footprint pilot phase on the way to a single market for green products in the European Union, Prog. Photovolt.: Res. Appl. **26**, 553 (2018). https://doi.org/10.1002/pip.2956

37. J. Zhang, X. Gao, Y. Deng, Y. Zha, C. Yuan, Comparison of life cycle environmental impacts of different perovskite solar cell systems, Sol. Energy Mater. Sol. Cells **166**, 9 (2017). https://doi.org/10.1016/j.solmat.2017.03.008
38. S. Maranghi, M.L. Parisi, R. Basosi, A. Sinicropi, The critical issue of using lead for sustainable massive production of perovskite solar cells: a review of relevant literature, Open Res. Eur. **1**, 44 (2021). https://open-research-europe.ec.europa.eu/articles/1-44/v2
39. J.A. Alberola-Borràs, R. Vidal, E.J. Juárez-Pérez, E. Mas-Marzá, A. Guerrero, I. Mora-Seró, Relative impacts of methylammonium lead triiodide perovskite solar cells based on life cycle assessment, Sol. Energy Mater. Sol. Cells **179**, 169 (2018). https://doi.org/10.1016/j.solmat.2017.11.008
40. T. Okoroafor, A. Maalouf, S. Oez, V. Babu, B. Wilk, S. Resalati, Life cycle assessment of inkjet printed perovskite solar cells, J. Clean. Prod. **373**, 133665 (2022). https://doi.org/10.1016/j.jclepro.2022.133665
41. M. Krebs-Moberg, M. Pitz, T.L. Dorsette, S.H. Gheewala, Third generation of photovoltaic panels: a life cycle assessment, Renew. Energy **164**, 556 (2021). https://doi.org/10.1016/j.renene.2020.09.054
42. L. Vesce et al., Perovskite solar cell technology scaling-up: Eco-efficient and industrially compatible sub-module manufacturing by fully ambient air slot-die/blade meniscus coating, Prog. Photovolt.: Res. Appl. **32**, 115 (2023). https://doi.org/10.1002/pip.3741
43. L. Vesce et al., Ambient air blade-coating fabrication of stable triple-cation perovskite solar modules by green solvent quenching, Solar RRL **5**, 2100073 (2021), https://doi.org/10.1002/solr.202100073
44. H. Chen et al., A solvent-and vacuum-free route to large-area perovskite films for efficient solar modules, Nature **550**, 92 (2017). https://doi.org/10.1038/nature23877
45. M. Yang et al., Highly efficient perovskite solar modules by scalable fabrication and interconnection optimization, ACS Energy Lett. **3**, 322 (2018). https://doi.org/10.1021/acsenergylett.7b01221
46. ISO 14040 Environmental management-Life cycle assessment-Principles and framework Management environnemental. https://www.iso.org/standard/37456.html
47. ISO 14044 Environmental management-Life cycle assessment-Requirements and guidelines (2006). https://www.iso.org/standard/38498.html
48. E. Moreno Ruiz et al., *Documentation of changes implemented in the ecoinvent database v3.7 & v3.7.1* (ecoinvent Association, Zürich, Switzerland, 2020)
49. S. Maranghi, M.L. Parisi, R. Basosi, A. Sinicropi, Environmental profile of the manufacturing process of perovskite photovoltaics: harmonization of life cycle assessment studies, Energies **12**, 3746 (2019). https://doi.org/10.3390/en12193746
50. M. Bidikoudi, C. Simal, E. Stathatos, Low-toxicity perovskite applications in carbon electrode perovskite solar cells—a review, Electronics **10**, 1145 (2021). https://doi.org/10.3390/electronics10101145
51. K. Lee et al., A highly stable and efficient carbon electrode-based perovskite solar cell achieved via interfacial growth of 2D PEA2PbI4 perovskite, J. Mater. Chem. A **6**, 24560 (2018). https://doi.org/10.1039/C8TA09433K
52. C. Zhou, S. Lin, Carbon-electrode based perovskite solar cells: effect of bulk engineering and interface engineering on the power conversion properties, Solar RRL **4**, 1900190 (2019). https://doi.org/10.1002/solr.201900190
53. M. Que, B. Zhang, J. Chen, X. Yin, S. Yun, Carbon-based electrode for perovskite solar cells, Mater. Adv. **2**, 5560 (2021). https://doi.org/10.1039/d1ma00352f
54. A. Mei et al., A hole-conductor-free, fully printable mesoscopic perovskite solar cell with high stability, Science **345**, 295 (2014). https://doi.org/10.1126/science.1254763
55. L. Cai, L. Liang, J. Wu, B. Ding, L. Gao, B. Fan, Large area perovskite solar cell module, J. Semicond. **38**, 014006 (2017). https://doi.org/10.1088/1674-4926/38/1/014006
56. H. Wei et al., Free-standing flexible carbon electrode for highly efficient hole-conductor-free perovskite solar cells, Carbon **93**, 861 (2015). https://doi.org/10.1016/j.carbon.2015.05.042
57. H. Zhang et al., Self-adhesive macroporous carbon electrodes for efficient and stable perovskite solar cells, Adv. Funct. Mater. **28**, 1802985 (2018). https://doi.org/10.1002/adfm.201802985
58. P. Kartikay, D. Sadhukhan, A. Yella, S. Mallick, Enhanced charge transport in low temperature carbon-based n-i-p perovskite solar cells with NiOx-CNT hole transport material, Sol. Energy Mater. Sol. Cells **230**, 111241 (2021). https://doi.org/10.1016/j.solmat.2021.111241
59. R. Tsuji et al., Function of porous carbon electrode during the fabrication of multiporous-layered-electrode perovskite solar cells, Photonics **7**, 133 (2020). https://doi.org/10.3390/photonics7040133
60. H. Zhang et al., High-efficiency (>20%) planar carbon-based perovskite solar cells through device configuration engineering, J. Colloid Interface Sci. **608**, 3151 (2022). https://doi.org/10.1016/j.jcis.2021.11.050
61. M. Li et al., Nickel-doped graphite and fusible alloy bilayer back electrode for vacuum-free perovskite solar cells, ACS Energy Lett. **8**, 2940 (2023). https://doi.org/10.1021/acsenergylett.3c00852
62. S.N. Habisreutinger, T. Leijtens, G.E. Eperon, S.D. Stranks, R.J. Nicholas, H.J. Snaith, Carbon nanotube/polymer composites as a highly stable hole collection layer in perovskite solar cells, Nano Lett. **14**, 5561(2014). https://doi.org/10.1021/nl501982b
63. X. Li, F. Zhang, H. He, J.J. Berry, K. Zhu, and T. Xu, On-device lead sequestration for perovskite solar cells, Nature **578**, 555 (2020). https://doi.org/10.1038/s41586-020-2001-x
64. C. Chen, S. Cheng, L. Cheng, Z. Wang, L. Liao, Toxicity, leakage, and recycling of lead in perovskite photovoltaics, Adv. Energy Mater. **13**, 2204144 (2023). https://doi.org/10.1002/aenm.202204144
65. R.D. Mendez, B.N. Breen, D. Cahen, Lead sequestration from halide perovskite solar cells with a low-cost thiol-containing encapsulant, ACS Appl. Mater. Interfaces **14**, 29766 (2022). https://doi.org/10.1021/acsami.2c05074
66. M.L. Parisi, A. Sinicropi, Closing the loop for perovskite solar modules, Nat. Sustain. **4**, 754 (2021). https://doi.org/10.1038/s41893-021-00735-1
67. H. Luo, P. Li, J. Ma, X. Li, H. Zhu, Y. Cheng, Q. Li, Q. Xu, Y. Zhang, Y. Song, Bioinspired cage traps for closed-loop lead management of perovskite solar cells under real-world contamination assessment, Nat. Commun. **14**, 4730 (2023). https://doi.org/10.1038/s41467-023-40421-8
68. M.Z. Mokhtar, J. He, M. Li, Q. Chen, J.C. Ren K., D.J. Lewis, A.G. Thomas, B.F. Spencer, S.A. Haque, B.R. Saunders, Bioinspired scaffolds that sequester lead ions in physically damaged high efficiency perovskite solar cells, Chem. Commun. **57**, 994 (2021). https://doi.org/10.1039/d0cc02957b
69. X. Li, F. Zhang, H. He, J.J. Berry, K. Zhu, T. Xu, On-device lead sequestration for perovskite solar cells, Nature **578**, 555 (2020). https://doi.org/10.1038/s41586-020-2001-x
70. A. Gargiulo, M.L. Carvalho, P. Girardi, Life cycle assessment of Italian electricity scenarios to 2030, Energies **13**, 3852 (2020). https://doi.org/10.3390/en13153852
71. A. Gargiulo, P. Girardi, G. Mela, Life Cycle Assessment della produzione di energia elettrica nazionale attuale ed al 2030 (2019). https://www.rse-web.it/rapporti/19012876/#

Cite this article as: Federico Rossi, Leonardo Rotondi, Maurizio Stefanelli, Adalgisa Sinicropi, Luigi Vesce, Maria Laura Parisi, Comparative life cycle assessment of different fabrication processes for perovskite solar mini-modules, EPJ Photovoltaics 15, 20 (2024)